

# Morphology and electrochemical behavior of an ultrafine $\text{LiMn}_2\text{O}_4$ powder obtained by a new route, from freeze-dried precursors

T. Le Mercier,<sup>\*a</sup> J. Gaubicher,<sup>a</sup> E. Bermejo,<sup>a</sup> Y. Chabre<sup>b</sup> and M. Quarton<sup>a</sup>

<sup>a</sup>Laboratoire de Cristallochimie du Solide, CNRS-URA 1388, Université Pierre et Marie Curie, 4 place Jussieu, 75252 Paris Cedex 05, France. E-mail: lemercier@ccr.jussieu.fr

<sup>b</sup>Laboratoire de Spectrométrie Physique, Université Joseph Fourier-Grenoble I, and CNRS, BP 87, 38402 Saint Martin d'Hères, France

Received 6th July 1998, Accepted 14th October 1998

An ultrafine (25–40 nm) powder of spinel lithium manganese oxide with composition  $\text{Li}_{0.95}\text{Mn}_2\text{O}_4$  was obtained from decomposition of freeze drying nitrate precursors and heat treatment below 500 °C. Positive electrodes prepared with this material have been cycled between 4.6 and 3.1 V up to C/2 rate. The specific discharge capacity at such a rate decreases from 110 to 90 mA h g<sup>-1</sup> after 80 cycles, with a low polarization only.

## 1 Introduction

Rechargeable lithium batteries are under intensive development worldwide as a consequence of their high gravimetric and volumetric energy densities. Among the positive electrode materials presently considered, manganese oxides are cheaper and less toxic than cobalt, nickel or vanadium oxides.<sup>1</sup> Thus, several lithium manganese oxides have been investigated for electrochemical applications, notably the spinel  $\text{LiMn}_2\text{O}_4$ .<sup>2,3</sup> Most of the lithium can be reversibly removed from this compound in the range 4 V vs.  $\text{Li}^+/\text{Li}^0$  which makes it suitable for Li-ion batteries.<sup>4</sup> In order to improve cycling performances, several low temperature routes were developed such as sol-gel<sup>5</sup> co-precipitation,<sup>6</sup> aqueous route<sup>7–9</sup> and Pechini process<sup>10</sup> which allowed powders to be obtained with small average particle size. Freeze-drying, another technique used to prepare fine particles, appears more suitable because it eliminates some drawbacks inherent to the above techniques of powder synthesis (e.g. difficulty in controlling the gel drying step, the high cost of some reactants). In addition to the fact that freeze drying is an easy and cheap procedure (low cost of apparatus and of nitrates which are most frequently used as the initial reagents) the main advantages of this cryochemical route are the greater purity and homogeneity of the powders and the smaller particle dimensions of the end-product. It provides the possibility to obtain powder mixtures with large-surface area that can react at temperatures significantly below those required for more conventional powders.<sup>11</sup> Recently, we have shown the possibility to synthesize a ferrite spinel using this original route.<sup>12</sup> The essence of the freeze-drying technique consists of the following steps:

(1) The salts are mixed in solution and the homogeneity is maintained by the virtually instant freezing of sprayed micro-drops and (2) the droplets are then dehydrated by sublimation.

The thermal treatment of the cryogranulates allows pure and stable homogeneous products to be obtained. Thus, this present work deals with the preparation by freeze-drying and the electrochemical studies of ultrafine particles of lithium manganese spinel oxide.

## 2 Experimental

A stoichiometric mixture was prepared from reagent grade lithium nitrate ( $\text{LiNO}_3$ ) and manganese nitrate hexahydrate [ $\text{Mn}(\text{NO}_3)_2 \cdot 6\text{H}_2\text{O}$ ]. These nitrates were preferred to other salts because of their lower temperature of decomposition (below 200 °C) thus preventing a loss of the fine particle

nature by increase of grain size during heat treatment. In order to obtain high purity starting compounds, 99.99% pure and distilled water was used. To obtain freeze-dried precursors of  $\text{LiMn}_2\text{O}_4$  powder a process with three main stages was carried out.

First, a solution containing salts in stoichiometric proportions to give 15 g of powder per liter of solution was filtered to remove any undissolved impurities, then sprayed as an aerosol into a dish containing liquid nitrogen, which induced rapid freezing of the droplets.

Secondly, the sprayed droplets, ranging in size from 100 to 300  $\mu\text{m}$ , were dried by sublimation. Vacuum (0.71 Pa) was maintained throughout the process to remove the water. Since the application of heat increases the rate of sublimation, an optimum rate of heat supply was determined empirically. The hot-plate temperature was brought from –30 up to 0 °C in 8 h and held for 15 h at 20 °C then 5 h at 90 °C to improve the dehydration and to avoid the deliquescence of the obtained powders.

Thirdly, because of the hygroscopicity of nitrate mixture, the powder was heated at 270 °C in an air flow for 10 min to convert the nitrates into oxides with release of nitrous steam.

Finally, in order to obtain  $\text{LiMn}_2\text{O}_4$ , an annealing treatment at low temperature is performed on freeze-dried precursors.

The Li/Mn ratio was determined by elemental chemical analysis and found to be  $0.475 \pm 0.005$ ; thus the formulation can be expressed as  $\text{Li}_{0.95}\text{Mn}_2\text{O}_4$ .

TEM photomicrographs were used to study the shape and the particle size and to estimate the state of agglomeration of the particles. For this, a small amount of powder was combined with ethanol and glycerol and placed in an ultrasonic bath prior to collection of the particles for the TEM experiments.

X-Ray diffraction (XRD) measurements were carried out at room temperature using a Philips diffractometer operating with  $\text{Cu-K}\alpha$  radiation ( $\lambda_{\text{K}\alpha} = 1.54059 \text{ \AA}$ ) on powders before and after heat treatment in air at various temperature for 1 h.

Thermal studies were carried out using a simultaneous DTA–TG thermal analyzer model SETARAM 92. All measurements were performed in air with 10 °C min<sup>-1</sup> heating or cooling rate.

Electrochemical intercalation studies were carried out in both potentiodynamic and galvanostatic modes using a MacPile system<sup>13</sup> and Swagelok<sup>®14</sup> type cells, assembled in a dry-box, with Li metal as the negative electrode and 1 M  $\text{LiClO}_4$  [ethylene carbonate (EC)–dichloromethane (DCM)] as the electrolyte. Composite positive electrodes were made of 12wt% of polyvinylidene fluoride (PVDF), 8wt% of acetylene

black (4N, Strem Chemicals) as electronic binder and 80wt% of  $\text{LiMn}_2\text{O}_4$ . These powders were mixed, ground in an agate mortar or as specified further in a planetary ball milling and then suspended in cyclopentanone. Typically 20 mg of the resulting mixture was deposited on a stainless steel disk of  $1 \text{ cm}^2$  and then dried under vacuum at  $80^\circ\text{C}$ .

The powders were characterized by BET surface area analysis in nitrogen according to the three-point method.

### 3 Results and discussion

Fig. 1 shows the DTA–TG plots recorded on the powder obtained after freeze-drying. Two broad endothermic peaks corresponding to weight losses are visible at *ca.*  $60^\circ\text{C}$  (14wt%) and  $270^\circ\text{C}$  (20wt%) respectively. No DTA–TG peak appears during cooling and after heating to  $900^\circ\text{C}$ , XRD confirmed that the powder is a pure phase with a spinel type structure. In order to characterize the chemical evolution of the mixture, XRD patterns have been recorded on freeze-dried powders at room temperature and after annealing for 1 h at temperatures corresponding to the different domains defined by the TG analysis:  $140^\circ\text{C}$ ,  $360^\circ\text{C}$  and  $480^\circ\text{C}$  (Fig. 2). The room temperature XRD pattern is characteristic of an amorphous sample. After annealing at  $140^\circ\text{C}$ , two phases can be separated:  $\text{LiNO}_3$  with a good crystallinity (narrow peaks) and probably manganese oxide (broad peaks). For an annealing temperature of  $360^\circ\text{C}$ , the diffraction lines of lithium nitrate had vanished, and only the broad peaks remain. Thus, the second weight loss probably corresponds to release of  $\text{NO}_2$ . After annealing at  $480^\circ\text{C}$ , only the diffraction peaks of lithium manganese spinel can be observed. Thus, DTA–TG and XRD studies indicate water losses between  $60$  and  $120^\circ\text{C}$  and  $\text{NO}_2$  losses between  $270$  and  $360^\circ\text{C}$ . Simultaneously, phase transitions can occur at *ca.*  $40$  and  $240^\circ\text{C}$ . The main result is the formation of the spinel phase between  $360$  and  $480^\circ\text{C}$ .

The experimental value of the cubic cell parameter of  $\text{Li}_{0.95}\text{Mn}_2\text{O}_4$  obtained after annealing at  $480^\circ\text{C}$  and refined by least square methods is:  $a=8.236(1) \text{ \AA}$ . This value is slightly lower than for crystalline  $\text{LiMn}_2\text{O}_4$  ( $a=8.242 \text{ \AA}$ ). This is in agreement with a Li/Mn ratio lower than 0.5.<sup>15</sup> Moreover the Mn oxidation state has been determined by redox titration to 3.52(2).

As shown in the insert in Fig. 2, the diffraction peaks are much broader in the case of the freeze-drying product than for the compound obtained by a classical route (calcination of powders in air at  $800^\circ\text{C}$  during 24 h). Assuming that the peaks broadening is only due to the particle size factor, an

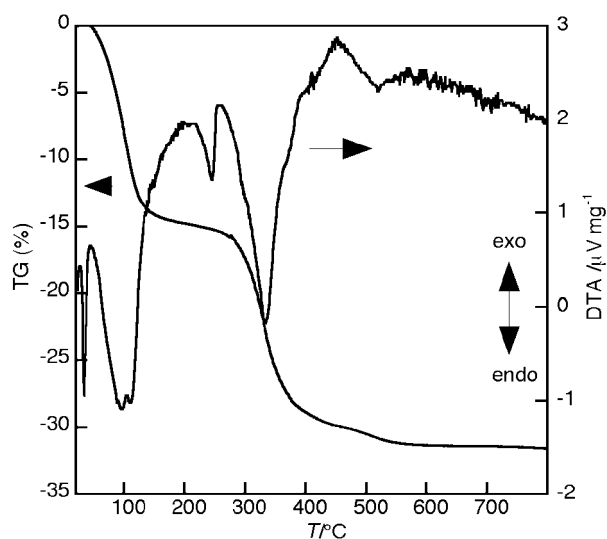


Fig. 1 DTA/TG curves of  $\text{Li}_{0.95}\text{Mn}_2\text{O}_4$  powder after freeze-drying under air.

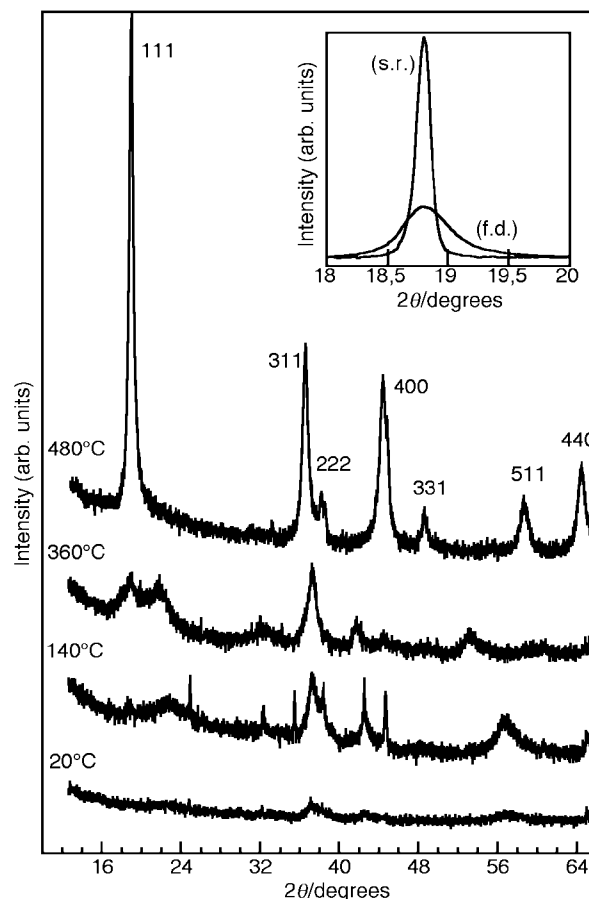


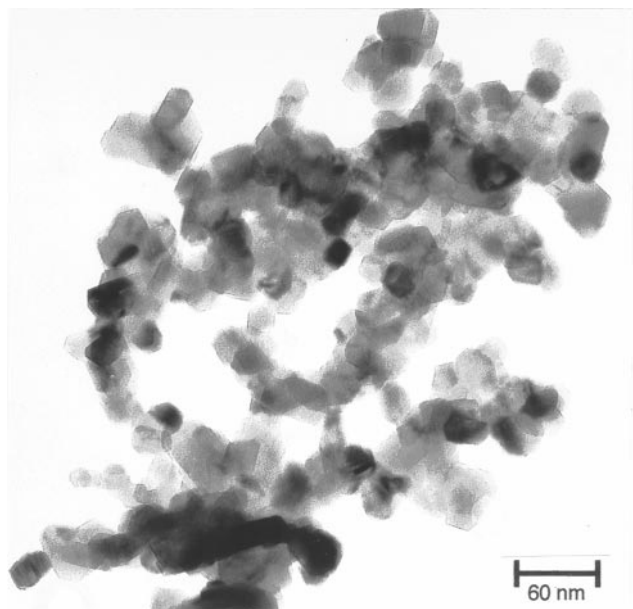
Fig. 2 XRD patterns of the freeze-dried powder after annealing during 1 h. The insert compares the (111) diffraction peak of spinel synthesized by solid route (s.r.) and freeze-drying (f.d.).

average size was obtained from Scherrer's formula. A mono-disperse tungsten carbide WC powder was used as internal standard in order to take into account of the intrinsic broadening due to the measurement system. The average size of the  $\text{Li}_{0.95}\text{Mn}_2\text{O}_4$  particles obtained from freeze-drying precursors was determined to be 34 nm.

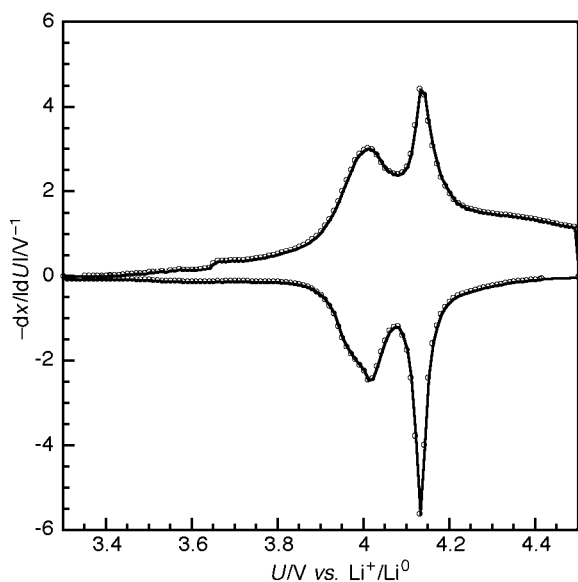
In order to check this result, TEM micrography observations have been performed on powders after annealing for 1 h at  $480^\circ\text{C}$  (Fig. 3). Small nearly spherical particles were revealed with a narrow size distribution from 25 to 40 nm, consistent with the XRD result. Most of these particles appeared as small crystals with morphology limited by plane faces. The BET surface area ( $24 \text{ m}^2 \text{ g}^{-1}$ ) was higher than that measured for  $\text{LiMn}_2\text{O}_4$  obtained by other methods ( $3\text{--}11 \text{ m}^2 \text{ g}^{-1}$ ).<sup>16,17</sup>

Fig. 4 shows a typical incremental capacity voltammogram, obtained for the first cycle from a stepwise potentiodynamic cycling with  $\pm 10 \text{ mV}$  steps every 3 h within a 3.3–4.5 V potential window. The 'dried-freeze  $\text{Li}_{0.95}\text{Mn}_2\text{O}_4\text{-Li}$ ' system presents the classical two steps occurring near 4.0 and 4.1 V characteristic of manganese oxide spinel electrochemical behavior. These two steps are well resolved and appear at the same respective potentials upon the reduction and the corresponding oxidation. This is typically the signature of a fast intercalation–deintercalation kinetic process. It should be noticed that the oxidation peak near 4.0 V is relatively broad compared to that at 4.1 V. As described elsewhere<sup>18</sup> this has been attributed, in the case of  $\text{LiMn}_2\text{O}_4$ , to the fact that the oxidation peak near 4.0 V corresponds to a solid solution process, whereas that at 4.1 V is associated to a phase transition.

In terms of application and to get a better insight of the electrochemical performances, the cycling behavior of this system has also been investigated in galvanostatic mode at



**Fig. 3** TEM image of an agglomerate of lithium manganese spinel oxide freeze-dried particles.



**Fig. 4** Voltammogram of incremental capacity obtained from potentiodynamic cycling of  $\text{Li}_{0.95}\text{Mn}_2\text{O}_4$  with 10 mV/3 h potential steps and curtailing condition equivalent to C/1000.

several regimes from C/10 to C/2 (meaning that the nominal capacity is reached within 10 to 2 h respectively) within a 3.1–4.6 V potential window. A typical capacity curve as a function of the number of cycles is shown on Fig. 5. The discharged capacity retention is excellent, decreasing from 105 to 95  $\text{mA h g}^{-1}$  after almost 90 cycles. By comparison with published results<sup>5,7,19</sup> where the manganese oxide spinel has been synthesized at low temperature (below 500 °C) such a capacity retention is so far the highest encountered. Twenty subsequent cycles at higher regime (C/5) do not strongly affect the system capacity. In fact, this increase of regime results in a capacity fading from 97 to 93  $\text{mA h g}^{-1}$ . When going back to a C/10 regime the previous capacity is recovered, indicating that the capacity fading is not due to the loss of active material resulting from breaking of the electronic contact between particles but arises from a kinetic limitation.

However the polarization which is 0.25 V at the C/10 regime increases drastically to 0.55 V when increasing the regime to

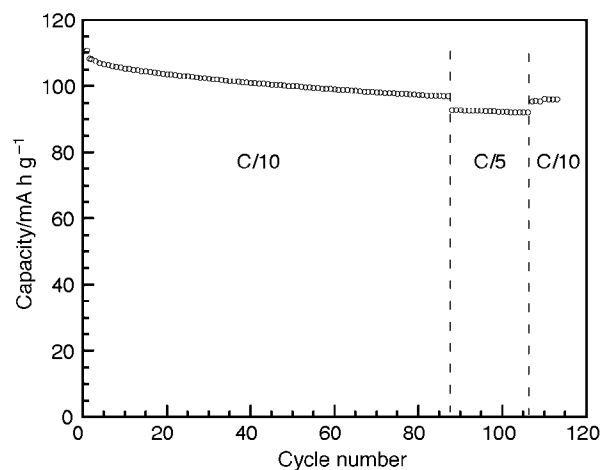


**Fig. 5** Variation of specific discharge capacity obtained from galvanostatic cycling of  $\text{Li}_{0.95}\text{Mn}_2\text{O}_4$  at C/10 and C/5 nominal regimes within a 4.6–3.1 V potential window.

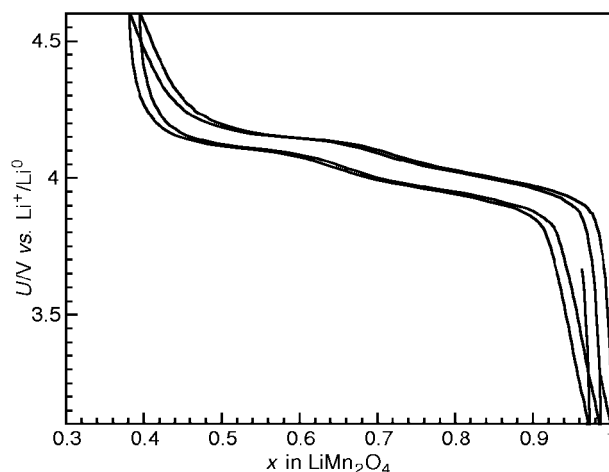


**Fig. 6** The two first cycles obtained at a C/2 nominal regime after 20 cycles at C/10 and 20 subsequent cycles at C/5 nominal regimes.

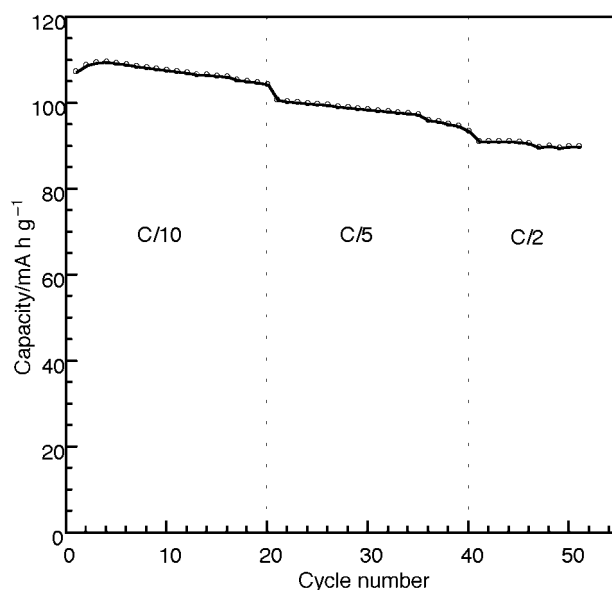


**Fig. 7** Variation of specific discharge capacity obtained from galvanostatic cycling of  $\text{Li}_{0.95}\text{Mn}_2\text{O}_4$  at C/10, C/5 and C/2 nominal regimes within a 4.6–3.1 V potential window.

C/5, presumably because of a poor contact of the active material with the carbon.

Thus further experiments were performed after a long grinding of all the cathode components in a planetary ball milling. Fig. 6 shows the two first cycles at C/2 after 20 cycles at C/10 and 20 cycles at C/5. The polarization is greatly decreased and reaches only 0.1 V. The resulting discharge capacity curve is presented in Fig. 7. The initial delivered capacity close to  $110 \text{ mA h g}^{-1}$  is slightly enhanced in comparison with the previous cycling experiment. However, it should be noted that contact of the nanometer-sized particles of  $\text{Li}_{0.95}\text{Mn}_2\text{O}_4$  with the carbon has to be further improved since the observed initial capacity corresponds to 75% of the theoretical one. The cyclability is excellent since the capacity remains above  $90 \text{ mA h g}^{-1}$  after 20 cycles at C/2, with only a small kinetic fading when increasing the cycling regime.

#### 4 Conclusion

Monodisperse nanometer-sized particles of  $\text{Li}_{0.95}\text{Mn}_2\text{O}_4$  spinel were prepared by a new route from decomposition of freeze drying nitrate precursors below  $500^\circ\text{C}$ . Composite cathodes prepared with this material exhibit very good cycling behavior (weak loss of capacity, very small value of polarization) at a discharge rate of C/2 and between 3.1 and 4.5 V.

#### Acknowledgements

T. Le Mercier is grateful to the Direction des Recherches, Etudes et Techniques (Délégation Générale pour l'Armement) for financial support via 94-1171A contract. We are indebted to C. Lacour (Ecole Supérieure de Physique et de Chimie Industrielles de la Ville de Paris) for technical contributions concerning the freeze-drying techniques, and to G. Rousse and C. Masquelier for the redox titration experiments.

#### References

- 1 M. M. Thackeray, P. J. Johnson, L. A. de Picciotto, P. G. Bruce and J. B. Goodenough, *Mater. Res. Bull.*, 1984, **19**, 179.
- 2 J. M. Tarascon and D. Guyomard, *J. Electrochim. Soc.*, 1991, **138**, 2864.
- 3 M. M. Thackeray, *Progress Solid State Chem.*, 1997, **25**, 1.
- 4 J. M. Tarascon and D. Guyomard, *Electrochim. Acta*, 1993, **38**, 1221.
- 5 P. Barboux, J. M. Tarascon and F. K. Shokoohi, *J. Electrochem. Soc.*, 1991, **94**, 185.
- 6 X. Qiu, X. Sun, W. Shen and N. Chen, *Solid State Ionics*, 1997, **93**, 335.
- 7 C. Tsang and A. Manthiran, *Solid State Ionics*, 1996, **89**, 305.
- 8 P. Strobel, S. Rohs and F. Le Cras, *J. Mater. Chem.*, 1996, **6**, 1591.
- 9 H. Huang and P. C. Bruce, *J. Electrochem. Soc.*, 1994, **141**, L106.
- 10 W. Liu, K. Kowal and G. C. Farrington, *J. Electrochem. Soc.*, 1996, **143**, 3590.
- 11 C. Lacour, F. Laher-Lacour, A. Dubon, M. Laguës and P. Mocaër, *Physica C*, 1990, **167**, 287.
- 12 E. Bermejo, M. Quarton and C. Lacour, *Mater. Res. Bull.*, 1994, **29**, 965.
- 13 C. Mouget and Y. Chabre, Multichannel Potentiostat Galvanostat 'MacPile', licensed from CNRS & UJF-Grenoble to Bio-Logic Co., 1 Ave. de l'Europe, F-38640 Claix.
- 14 J. M. Tarascon and D. Guyomard, *J. Electrochem. Soc.*, 1992, **139**, 937.
- 15 W. I. F. David, M. M. Thackeray, L. A. de Picciotto and J. B. Goodenough, *J. Solid State Chem.*, 1987, **67**, 316.
- 16 Z. Jiang and K. M. Abraham, *J. Electrochem. Soc.*, 1996, **143**, 1591.
- 17 T. Tsumura, A. Shimizu and M. Inagaki, *J. Mater. Chem.*, 1993, **3**, 995.
- 18 H. Abiko, M. Hibino and T. Kudoz, *Electrochem. Solid State Lett.*, 1998, **3**, 114.
- 19 M. N. Richard, E. W. Fuller and J. R. Dahn, *Solid State Ionics*, 1994, **73**, 81.

Paper 8/05178J